AD-A095 732 MARTIN MARIETTA LABS BALTIMORE MD F/G 11/6
THE DELAYED FRACTURE OF ALUMINUM ALLOYS.(U)
JAN 81 J R PICKENS, D VENABLES, J A GREEN N00014-74-C-0277
UNCLASSIFIED MML-TR-81-6C NL

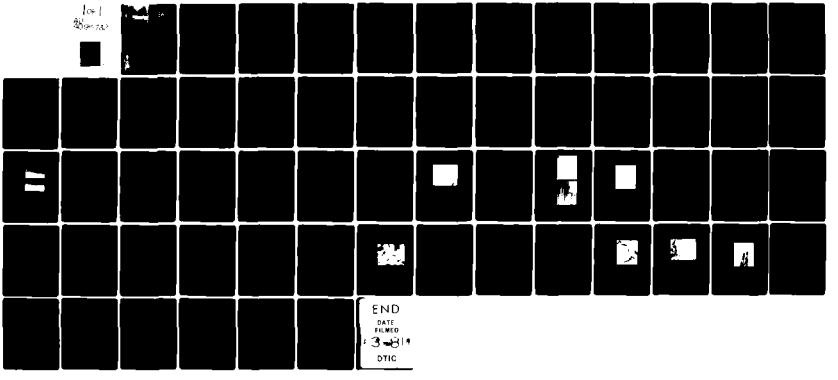

MARTIN MARIETTA

Martin Marietta Laboratories

12

LEVEL II

MML-TR-81-6c

THE DELAYED FRACTURE OF ALUMINUM ALLOYS

January 1981

Prepared by:
MARTIN MARIETTA CORPORATION
Martin Marietta Laboratories
1450 South Rolling Road
Baltimore, Maryland 21227

Prepared for Contract
N00014-74-C-0277 P00007
Office of Naval Research
Department of the Navy
800 North Quincy Street
Arlington, Virginia 22217

SECURITY CLASSIFICATION OF THIS PAGE *(When Data Entered)*

REPORT DOCUMENTATION PAGE

READ INSTRUCTIONS BEFORE COMPLETING FORM

1. REPORT NUMBER: MML TR 81-6c	2. GOVT ACCESSION NO.: AD-A095 732
3. RECIPIENT'S CATALOG NUMBER:	
4. TITLE *(and Subtitle)*: THE DELAYED FRACTURE OF ALUMINUM ALLOYS, End of Year Report	5. TYPE OF REPORT & PERIOD COVERED: End of year report (Jan. 1, 1980 to Dec. 31, 1980)
	6. PERFORMING ORG. REPORT NUMBER:
7. AUTHOR(s): Joseph R. Pickens, David Venables, John A.S. Green	8. CONTRACT OR GRANT NUMBER(s): N00014-74-C-0277, P00007
9. PERFORMING ORGANIZATION NAME AND ADDRESS: Martin Marietta Corporation, Martin Marietta Laboratories, 1450 S. Rolling Road, Baltimore, MD 21227	10. PROGRAM ELEMENT, PROJECT, TASK AREA & WORK UNIT NUMBERS:
11. CONTROLLING OFFICE NAME AND ADDRESS: Dept. of the Navy, Office of Naval Research, Code 471, Arlington, Virginia	12. REPORT DATE: January 1981
	13. NUMBER OF PAGES: 59
14. MONITORING AGENCY NAME & ADDRESS *(if different from Controlling Office)*:	15. SECURITY CLASS. *(of this report)*: Unclassified
	15a. DECLASSIFICATION DOWNGRADING SCHEDULE:

16. DISTRIBUTION STATEMENT *(of this Report)*

Distribution of this document is unlimited.

17. DISTRIBUTION STATEMENT *(of the abstract entered in Block 20, if different from Report)*

18. SUPPLEMENTARY NOTES

19. KEY WORDS *(Continue on reverse side if necessary and identify by block number)*

aluminum alloys, stress-corrosion cracking, oxide film, Auger electron spectroscopy, Auger depth profiling, intergranular fracture, thermal oxide aging curve, caustic etch process, tartaric acid anodizing, Mg/Zn, Mode I, Mode III

20. ABSTRACT *(Continue on reverse side if necessary and identify by block number)*

The fundamental mechanism of stress-corrosion cracking (SCC) has been studied for high-purity Al-Zn-Mg alloys. Earlier work at our laboratory and elsewhere established that hydrogen embrittlement is involved in the SCC mechanism. Moreover, we previously proposed that a Mg-H interaction exists that facilitates hydrogen entry into the alloy and its concentration at the grain boundary, leading to embrittlement. In the present work, we demonstrated the adverse effect of Mg in the bulk metal and in the oxide film on SCC. (continued)

DD FORM 1 JAN 73 1473 EDITION OF 1 NOV 65 IS OBSOLETE

SECURITY CLASSIFICATION OF THIS PAGE *(When Data Entered)*

20. Abstract (continued)

SCC testing of alloys whose surface oxide-films were removed so bulk composition effects could be studied, revealed that SCC susceptibility increases with increasing Mg to Zn wt% ratio. In film composition experiments, removal of the Mg-rich film that forms during heat treating, and replacing it with a Mg-free film by anodizing in tartaric acid decreased the susceptibility of an Al-Zn-Mg alloy. Moreover, susceptibility decreased with an increasing anodized-film thickness.

Fractographic studies revealed that pitting corrosion initiates intergranular SCC in these alloys.

MML TR 81-6c

THE DELAYED FRACTURE OF ALUMINUM ALLOYS

End of Year Report

January 1981

Prepared by:
J.R. Pickens, D. Venables, and J.A.S. Green
MARTIN MARIETTA CORPORATION
Martin Marietta Laboratories
1450 South Rolling Road
Baltimore, Maryland 21227

Prepared for:
Office of Naval Research
Department of the Navy
800 North Quincy Street
Arlington, Virginia 22217

Under Contract No. N00014-74-C-0277, P00007

ACKNOWLEDGEMENTS

Drs. Geoff Scammans and Clive Tuck were extremely helpful by providing their insights for the course of our research. We are also grateful to Professor Paul Paris for his many suggestions concerning our fracture toughness test systems. Mr. Bill Lauer's assistance in designing the precracking apparatus is greatly appreciated. We thank Mr. Charlie Brohawn for supplying the 5083 material.

Auger depth profiling was performed by Mr. Robert Butler under the auspices of Dr. T.S. Sun. Dr. Sun also performed the plasmon-loss energy experiment. Mr. David McNamara was helpful in obtaining and interpreting electron micrographs.

TABLE OF CONTENTS

LIST OF TABLES

LIST OF FIGURES

LIST OF FIGURES (Continued)

I. FOREWORD

This report presents the results of research performed March 1980 to January 1981 on the Office of Naval Research Contract No. N00014-74-C-0277, P00007.

II. BACKGROUND

Research at Martin Marietta Laboratories on the SCC of Al-Zn-Mg alloys has been ongoing for 14 years. Initial work focused on the dissolution mechanism of SCC[1-3] in which anodic dissolution in the grain boundary region serves as the principal mechanism of cracking. In the mid 1970's, this view was challenged,[4-8] and several investigators at Martin Marietta Laboratories[4] and elsewhere[5-8] provided strong evidence that hydrogen embrittlement (HE) is involved in the cracking mechanism.

Our group examined the effect of loading mode on the SCC susceptibility of 7075. Green et al.[4] found greater SCC susceptibility under Mode I loading (tension) than under Mode III loading (torsion) in an aqueous, chloride-containing environment. This indicates that HE is operating because the solubility of hydrogen in aluminum increases in a triaxial, tensile stress field,[9] which exists under Mode I, but not under Mode III loading. Since the triaxial, tensile stress field enables hydrogen to concentrate at the crack tip, embrittlement should be greater under Mode I loading than under Mode III loading when HE is operating. Green et al.[4] found this to be true (see Fig. 1).

They[4] then added arsenic, a hydrogen recombination poison, to the solution and found that the embrittlement under Mode I increased, but decreased under Mode III loading (Fig. 1). This was explained as follows. Under uniaxial tensile loading, where hydrostatic stresses force the concentration of hydrogen to a region of stress triaxiality ahead of the crack tip, the addition of arsenic retards the kinetics of hydrogen evolution and thereby increases hydrogen concentration within the metal, which in turn, enhances the hydrogen embrittlement of the aluminum alloy. Under torsional loading, however, there is insufficient hydrostatic stress to cause the localized concentration of hydrogen, and thus, the slower dissolution mechanism takes precedence. In this experiment, the arsenic served to retard the cathodic kinetics of the dissolution process, which under the acidic conditions known to exist

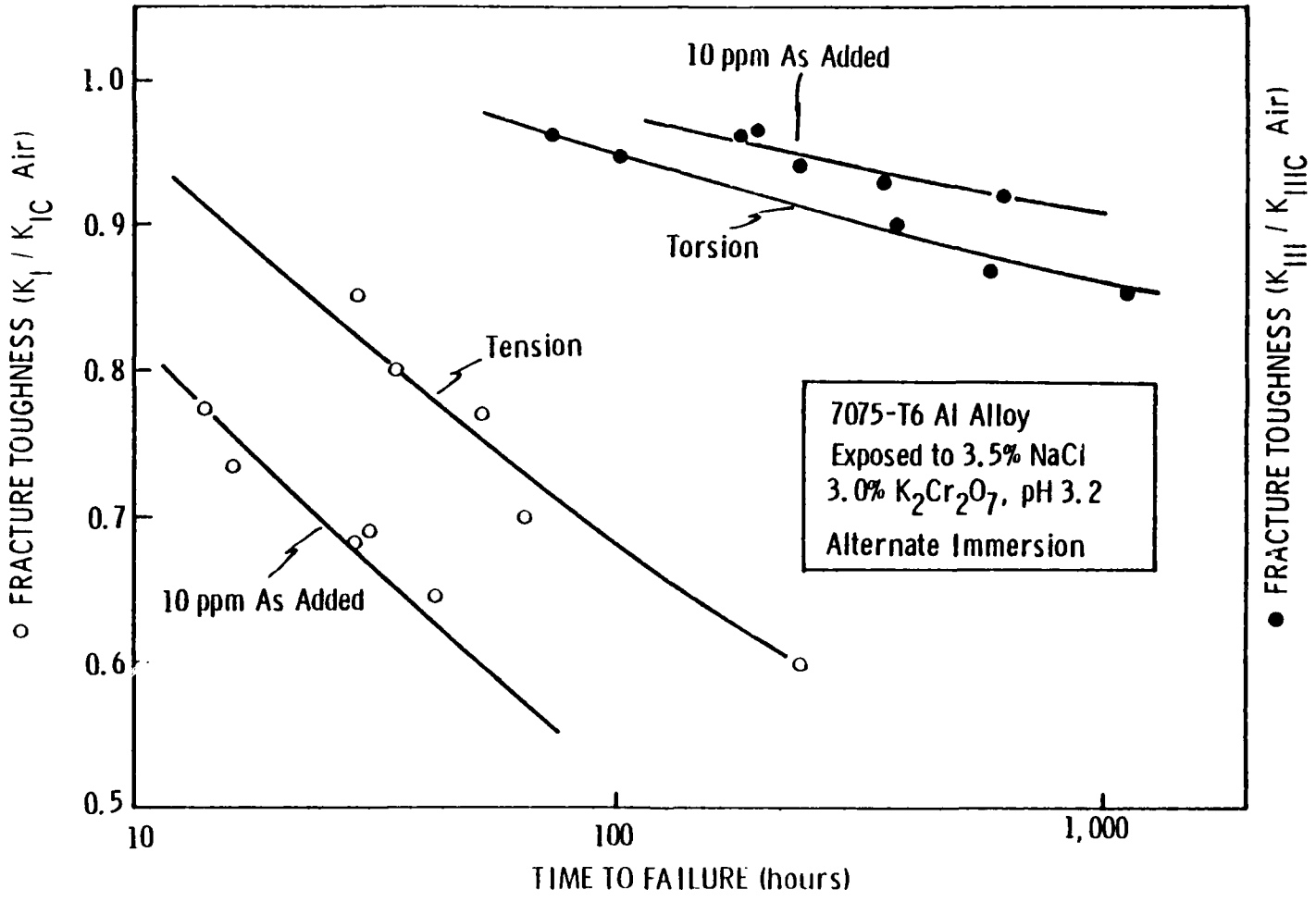

Figure 1. Susceptibility of 7075-T6 Al alloy to SCC in various saline solutions under both tensile and torsional loading.[4]

at tips of propagating cracks in aluminum alloys, is the recombination of hydrogen ions, i.e., $2H^+ + 2e^- \rightarrow H_2$. Therefore, susceptibility in Mode III decreases in the presence of arsenic.

With the advent of sophisticated surface analytical tools such as Auger electron spectroscopy (AES) and electron scattering for chemical analysis (ESCA), our effort was directed at studying the regions involved in SCC -- the oxide film and the grain boundary. We found that magnesium concentrates on the grain boundary in the as-quenched as well as the quenched-and-aged conditions.[10-11] Moreover, analysis of plasmon satellite-Auger peaks revealed that a substantial proportion of the grain-boundary magnesium is free,[12] i.e., not chemically bound. In addition, we found that magnesium segregates to the oxide film during solution heat treatment[12] and that the magnesium concentration is a sensitive function of the solution treatment temperature.[13] Interestingly, the solution treatment temperature for maximum Mg concentration in the film coincides with the temperature for maximum preexposure embrittlement found by Scamans et al.[14] These observations led us to speculate that a magnesium-hydrogen interaction is involved in the cracking mechanism.

Recent work by others[15,16] has provided indirect support for the proposed Mg-H interaction. For example, Tuck[15] used differential scanning calorimetry (DSC) to examine the decomposition of MgH_2 as a function of temperature. He located the decomposition peaks with respect to temperature and then performed similar DSC experiments on Al-5%Mg and Al-4.5%Zn-1.5% Mg alloys that were preexposed to water-vapor-saturated air. The agreement in peak location is fairly good, albeit with variations. His work provides strong indirect evidence that MgH_2 is present on the SCC fracture surfaces.

Additional indirect evidence of a Mg-H interaction was provided by Hidvégi and Kovács-Csetényi,[16] who performed evaporation studies on Al-Mg, Al-Zn, and various Al-Zn-Mg alloys by using mass-spectrometry. The evaporative loss was always greater than expected in the ternary alloys based on losses from the two binaries. Moreover, evaporative losses of hydrogen closely follow the losses of magnesium plus zinc.

They[16] explain this behavior by postulating the existence of a Zn-Mg-H complex in the alloy. Their result is consistent with our proposed Mg-H interaction, even though they claim that zinc also interacts with hydrogen.

In the past year, we performed experiments to demonstrate the harmful effects of magnesium and to seek evidence of the Mg-H interaction. The major experiments were to:

- Determine the effect of bulk composition on SCC susceptibility
- Control SCC susceptibility by controlling film composition
- Determine, by examining the effect of loading mode on susceptibility, whether commercial 5xxx alloys stress corrode by hydrogen embrittlement
- Identify the suspected Mg-H complex by examining the plasmon-loss satellite peaks of Auger electron spectroscopy.

As will be shown later, the results of some of these experiments suggested additional experiments that were performed during the past year.

III. RESULTS OF 1980 RESEARCH

A. EFFECT OF BULK COMPOSITION

1. Experimental Plan

To determine whether bulk magnesium content adversely affects susceptibility, we examined sheets of four high-purity Al-Zn-Mg alloys with different solute contents (wt% Zn + wt% Mg) and magnesium-to-zinc weight-percent ratios (Mg/Zn hereafter). Sheet tensile specimens were machined oriented in the longitudinal direction. All of these alloys have equiaxed grain structures, so orientation is not important. Aging curves were developed, and alloys were solution treated at 475°C, water quenched, and aged to similar (near peak) hardnesses. To eliminate the effects of variation in film composition, we removed the oxide films after heat treating by the procedure of Pistulka and Lang[17] (referred to as pickling hereafter). Then, we loaded specimens in tension in the acetic acid-brine solution of Pistulka and Lang[17] (see our previous report[18]) and generated stress vs time-to-failure (ttf) data.

2. Results

The pickling procedure successfully removed the oxide films,[19] which were enriched in magnesium from the solution-heat-treatment operation. Stress vs ttf data (see Fig. 2), show that susceptibility increases with increasing total solute content and with Mg/Zn.

3. Discussion

The increase in susceptibility with solute content is expected. However, the finding that susceptibility increases with increasing Mg/Zn at a constant solute content disagrees with some earlier work. Our result may help to resolve an existing controversy in the literature.

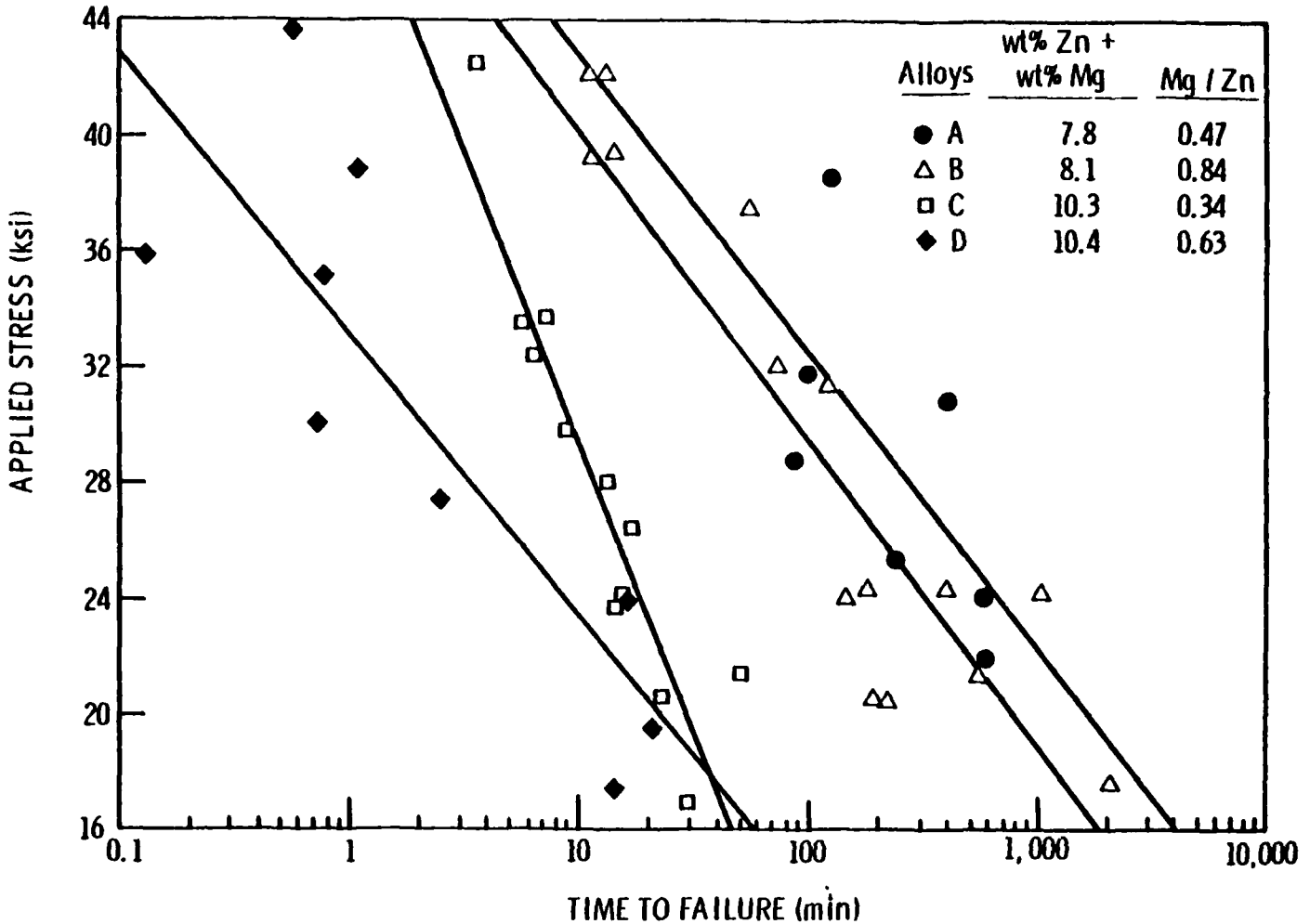

Figure 2. Stress vs time to failure for alloys of different bulk composition. Any effect of the oxide film on SCC susceptibility has been eliminated by removal of the film.

Some investigators have claimed that commercial Al-Zn-Mg alloys with low Mg/Zn produce greater strength and increased SCC susceptibility than alloys with high Mg/Zn.[20] In addition, Saxena et al.[21] claim that low Mg/Zn improves strength but impairs SCC resistance. Swann[22] discussed preliminary evidence that HE in 7xxx alloys may be related to Zn content and that aluminum alloys not containing Zn may be immune to cracking. These views are inconsistent with the results of our bulk composition experiments.

On the other hand, Staley[23] used a statistical analysis to correlate SCC behavior with the alloying content of experimental 7xxx alloys. He used the parameter MCYS (mean critical yield strength) as a measure of SCC resistance. The MCYS is the yield strength that gives an alloy a 50 percent probability of surviving two years in an industrial environment or 30 days in alternate immersion in a 3.5% NaCl aqueous solution, both at an applied stress of 241 MPa. Multiple regession analysis was performed to relate MCYS to the alloy contents of Zn, Mg, and Cu. Staley found the following equations.

Two years in an industrial environment:

$$MCYS = 65.4 + 0.43\ Zn - 4.84\ Mg + 6.88\ Cu$$

30 days in 3.5% NaCl alternate immersion:

$$MCYS = 63.8 + 0.64\ Zn - 2.96\ Mg + 4.22\ Cu.$$

Note that only Mg had an adverse (negative) effect on SCC resistance. Staley was contacted privately to comment on his results,[24] and claimed that of individual alloy pairs having constant copper content, those with higher Mg/Zn showed increased susceptibility. Staley's findings are consistent with our results for high purity Al-Zn-Mg alloys.

Ganguly and Dhindaw[25] also applied regression analysis to Al-Zn-Mg-Cu alloys to determine the effect of composition on SCC susceptibility. For constant copper content (1.5 wt%), they found that Mg had a much greater adverse effect on susceptibility than Zn. Moreover, they

found an interactive effect of Zn plus Mg that greatly promotes susceptibility. They attribute this synergism to the fact that $MgZn_2$-type compounds have a pronounced effect on susceptibility. To summarize, Ganguly and Dhindaw found that increasing Mg/Zn increases susceptibility.

The general trend in the development of newer 7xxx alloys with enhanced SCC resistance (e.g., 7050, 7049) has been towards lower Mg/Zn. This, along with the findings of Staley[23] and Ganguly and Dhindaw [25] is consistent with the findings of the present work.

The earlier work[20-22] showing that alloys had increased susceptibility with decreasing Mg/Zn may have led to this conclusion because the effects of film composition were not controlled. Viswanadham et al.[13] showed that slight changes in the temperature of solution heat treatment can greatly alter the Mg content of the oxide film. The results of our current work (discussed in section III.B) demonstrate that Mg content in the film greatly affects susceptibility. Thus, variations in the Mg content of the oxide films might account for the conflicting information in the literature.

To further elucidate the effect of Mg/Zn on SCC susceptibility, we separated Staley's data[24] into two groups, X and Y, based on impurity and copper content. Each group has similar compositions of Cu, Mn, Zr, and Fe, but different Mg/Zn. The MCYS was plotted vs Mg/Zn for each of the two groups, and further separation was noted based on the corrosive medium (i.e., industrial atmosphere or 3.5 wt% NaCl alternate immersion). Linear regressions of the four sets of data are plotted in Fig. 3. Despite the scatter, which is surprisingly low considering the "armchair" method by which we grouped the data, MCYS clearly decreases with increasing Mg/Zn.

We have demonstrated the adverse effect of bulk Mg content on SCC susceptibility. Our results are consistent with the suggestion of Viswanadham et al.[11] that a Mg-H interaction is involved in the SCC of Al-Zn-Mg alloys. Unfortunately, they do not provide direct evidence of a Mg-H interaction, but do have interesting practical applications.

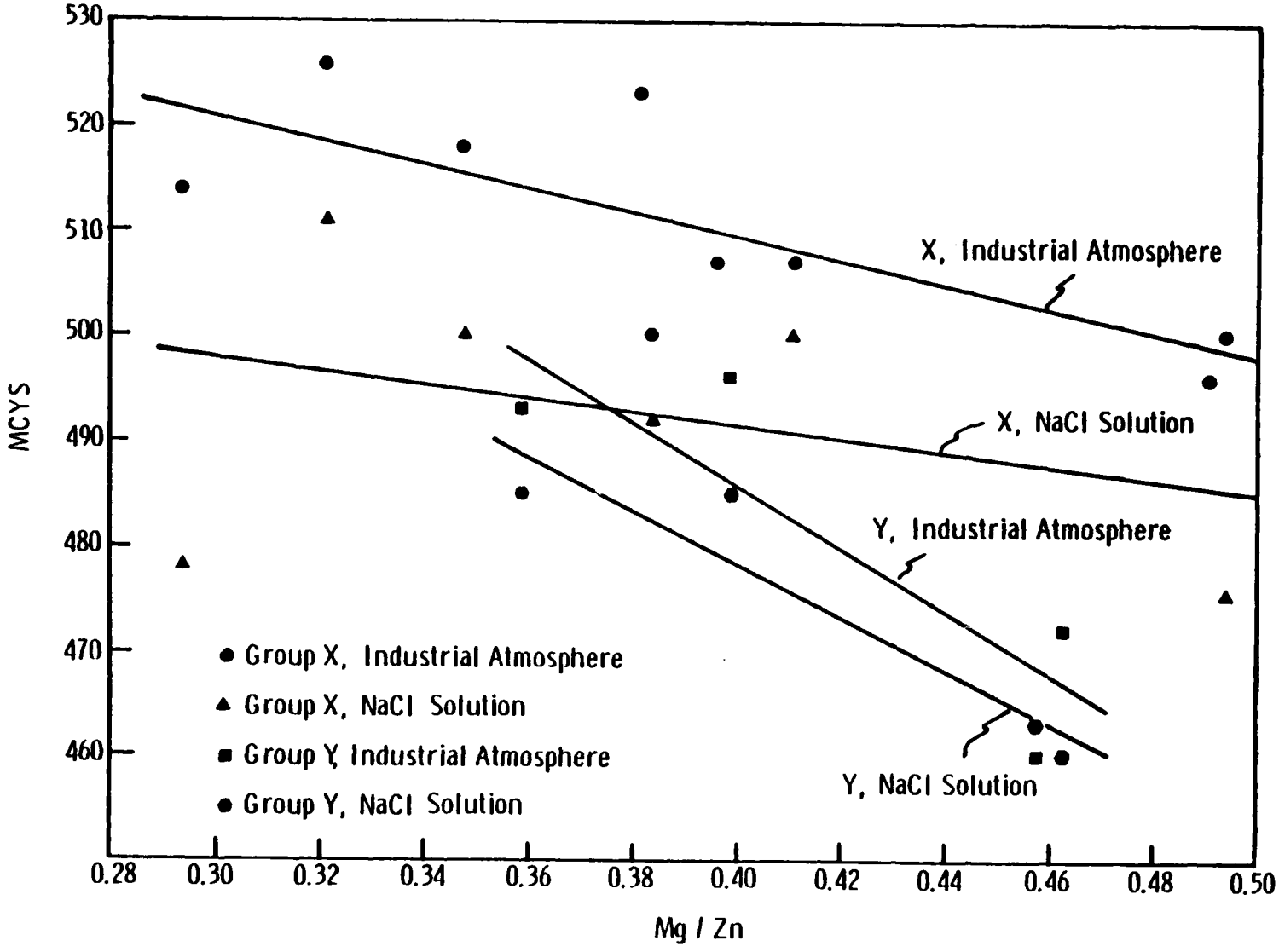

Figure 3. Mean critical yield stress vs Mg/Zn for Staley's data,[23] plotted after the data have been placed in groupings of similar composition of Cu and impurities.

The results suggest that Mg/Zn could be decreased, which still permits heat treatment to high strength levels, and the resulting alloy will have decreased SCC susceptibility.

B. EFFECT OF FILM COMPOSITION

We have shown[13] that magnesium segregates into the oxide film during solution heat treatment. The oxide film is clearly an alloy's first defense against SCC. Thus, if magnesium adversely affects SCC resistance by a Mg-H interaction, magnesium enrichment in the film would decrease SCC resistance. It is our aim to remove the magnesium-enriched "thermal" film and replace it with a magnesium-free film and thereby increase SCC resistance.

1. Experimental Plan

We examined several film removal techniques that could potentially remove aluminum and magnesium oxides -- the caustic etch (CE) procedure,[18,26] mechanical polishing, and mechanical polishing followed by tartaric acid anodizing (TAA).[27,28] (Table 1 gives the removal procedures.) Three alloys were subjected to the various removal techniques -- high purity Al-Zn-Mg alloys B and G, and commercial 7075. Their compositions and grain sizes are listed in Table 2. Sheet tensile specimens were machined in the long-transverse direction, polished to a 600-grit finish before heat treating, solution heat-treated, cold-water quenched, and aged to peak hardness. The aging curve for alloy B was obtained earlier,[18] and the curve for alloy G is given as Appendix A. Heat treating parameters are in Table 3.

We examined specimens of the three alloys, which had various oxide films as summarized in Table 4. Stress vs ttf data were generated in acetic acid-brine for these specimens.

Table 1

Film Removal Procedures

Pickling Procedure:

1. Wash in acetone
2. Pickle in 50 g HNO_3/liter for 1 hr at 30 ± 2°C
3. Rinse in distilled water
4. Etch in 100 g NaOH/liter for 1 min at 65 ± 1°C
5. Rinse in distilled water
6. Pickle in 50 g HNO_3/liter for 1 min at 30 ± 2°C
7. Rinse in distilled water
8. Wash in acetone
9. Dry at room temperature for 5 min
10. Store in silica gel desiccator

Caustic Etch Process:

1. Clean ultrasonically in acetone
2. Etch in 1 N NaOH (pH ~ 13.3) for 20 min at room temperature
3. Rinse in distilled water
4. Immerse in 10% HNO_3 (by volume; pH ~ 1.0) for 1 min
5. Rinse in distilled water
6. Place in vacuum (~ 700 torr) desiccator for ~ 35 min

Mechanical Removal:

1. Polish specimen with 600-grit paper
2. Polish edges with 2/0 emery paper
3. Rinse in distilled water
4. Clean ultrasonically in acetone
5. Rinse in distilled water
6. Clean ultrasonically in distilled water
7. Blow dry

Tartaric Acid Anodization Procedure:

1. Prepare surface of specimen by the mechanical removal procedure described above
2. Prepare anodizing solution: 30 g tartaric acid in 1 liter distilled water
3. Immerse Al specimen (anode) and Pt (cathode) in agitated anodizing solution
4. Apply desired voltage (~ 14 Å/volt) until current decays to ~ 0 mA (~ 20 min)
5. Rinse specimen in distilled water
6. Blow dry

Table 2

Composition and Grain Size of Alloys

Alloy	wt% Zn	wt% Mg	wt% Cu	wt% Cr	Mean Grain Size (μm)		
					Section Normal to Long-Transverse Direction	Section Normal to Short-Transverse Direction	Section Normal to Longitudinal Direction
B	4.4	3.7	0	0	14 x 8	15 x 10	20 x 18
G	4.4	3.7	0	0	185 x 183	179 x 171	175 x 160
7075	5.6	2.5	1.6	0.23	36 x 12	41 x 41	41 x 17

Table 3

Heat Treating Parameters

Alloy	Solution Heat Treatment		Quench	Artificial Aging	
	Temperature (°C)	Time (hours)	Temperature (°C)	Temperature (°C)	Time (hours)
B	475	2.0	0° Water	150	16.0
G	475	2.0	0° Water	150	2.5
7075	482	2.0	0° Water	121	24.0

Table 4

Oxide Conditions Tested for Alloys

Alloy	Oxide Conditions Tested
B	Thermal
	Caustic etch
G	Thermal
	Caustic etch
	Polished
	Polished + tartaric acid anodizing
7075	Thermal
	Caustic etch

2. Results

The CE procedure, mechanical polishing, and polishing followed by TAA all removed the thermal films and replaced them with Mg-free, alumina films. Auger depth profiles show that the thermal film is magnesium enriched (Fig. 4) and that the magnesium was removed from a stripped film (Fig. 5) of alloy B. These profiles are typical of the effects of the three film removal techniques on each of the three alloys.

The thicknesses of the various oxide films were measured from Auger depth profiles. The intersection of the aluminum (increasing) and oxygen (decreasing) lines is taken as the position of the depth of the oxide-metal interface. This depth is used as a measure of the film thickness.

In some cases, a metallographic profile containing the cross section of the oxide was observed in the scanning mode of the STEM (scanning tranmission electron microscope) to measure film thickness (see Fig. 6). These STEM results agree well with the thickness measurements obtained from the depth profiles.

Figure 7 plots stress vs ttf data for specimens of alloy B having the thermal film and having the Mg-free film formed by the CE procedure. Although experimental scatter is high, specimens having the Mg-free film clearly have reduced susceptibility.

Figure 8 shows linear regressions of stress vs ttf data for alloy G specimens having three different films: formed after polishing (i.e., mechanically polished), polished and TAA, and thermal (Mg-rich). The mechanically polished specimens have Mg-free films that are only 25-Å thick, but are approximately as susceptible as specimens having 2,000-Å-thick thermal films. When the Mg-free film is grown to 2,000 Å by TAA, the ttf at a given stress level increases by a factor of two.

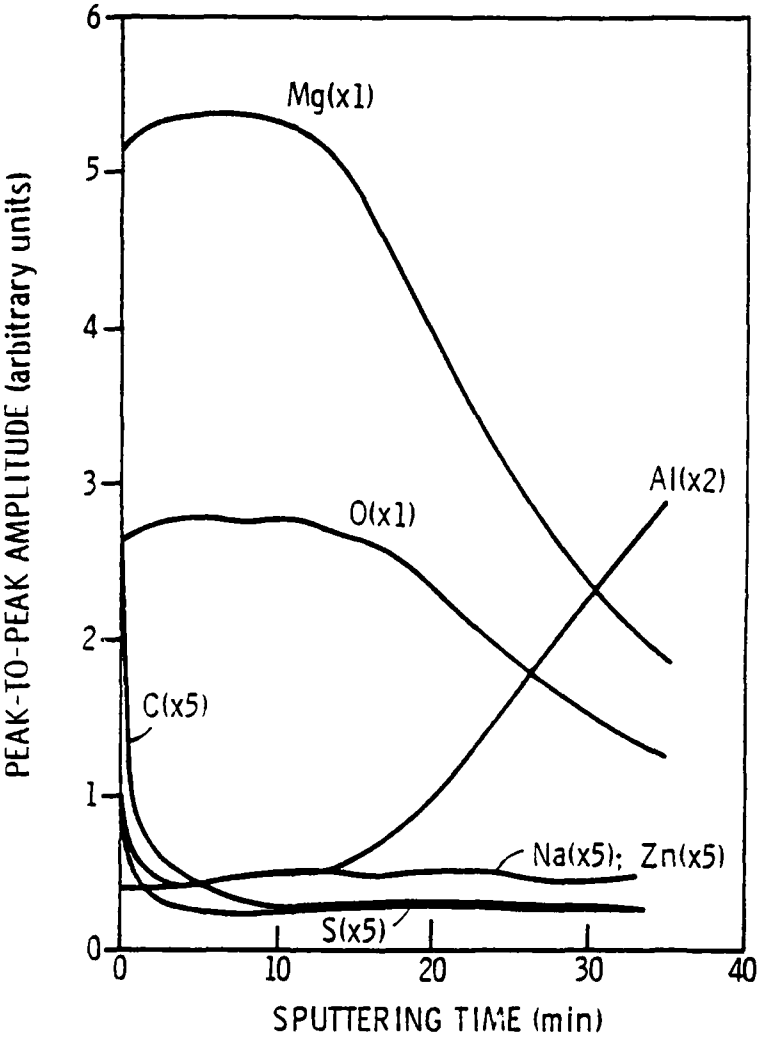

Figure 4. Auger depth profile of thermal film (Mg-rich).

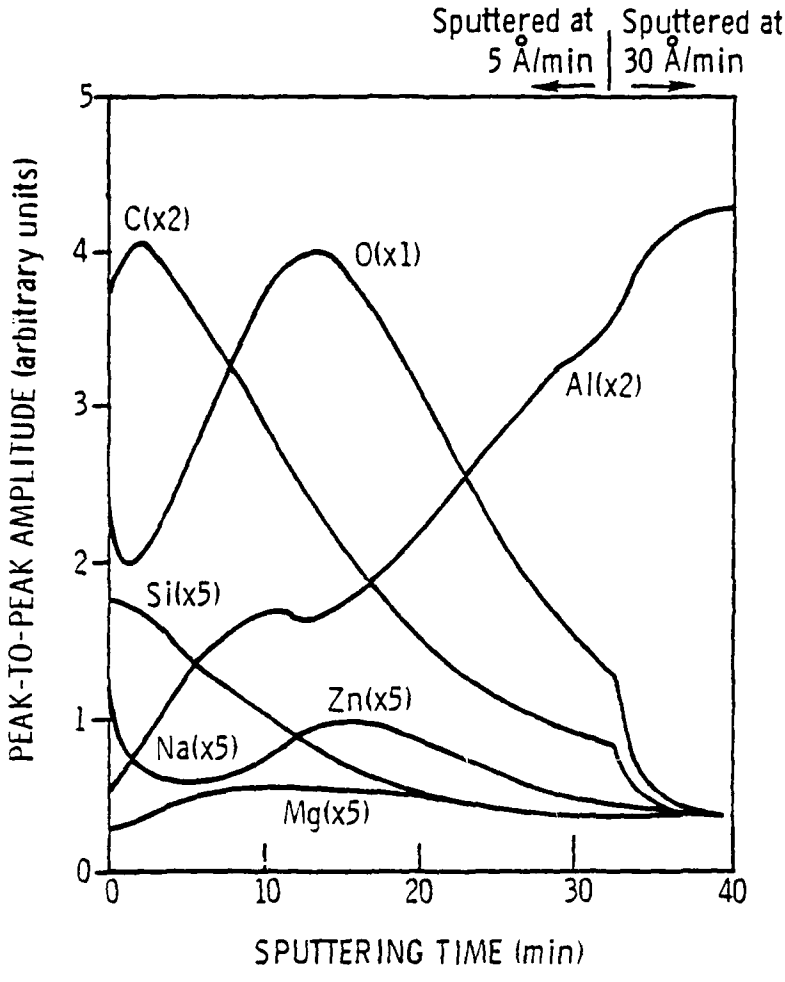

Figure 5. Auger depth profile of "naturally" formed film after film removal (essentially Mg-free).

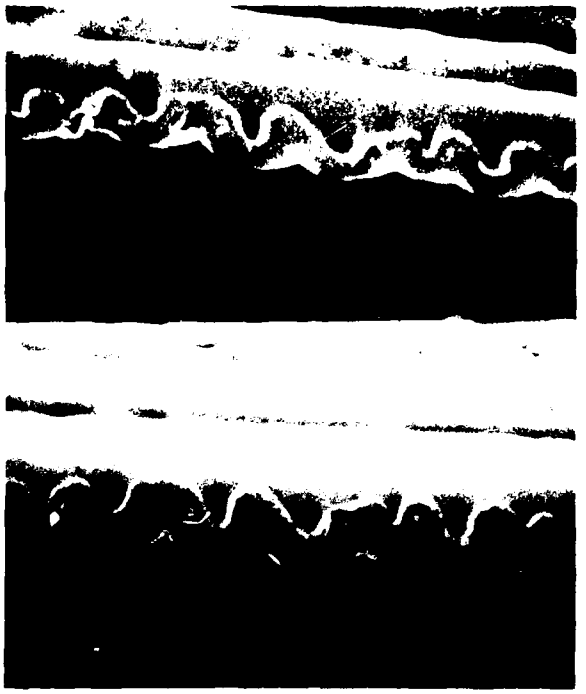

Figure 6. Stereo pair of an electron micrograph of alloy G showing the profile of the TAA film. (Magnification 40,000x.)

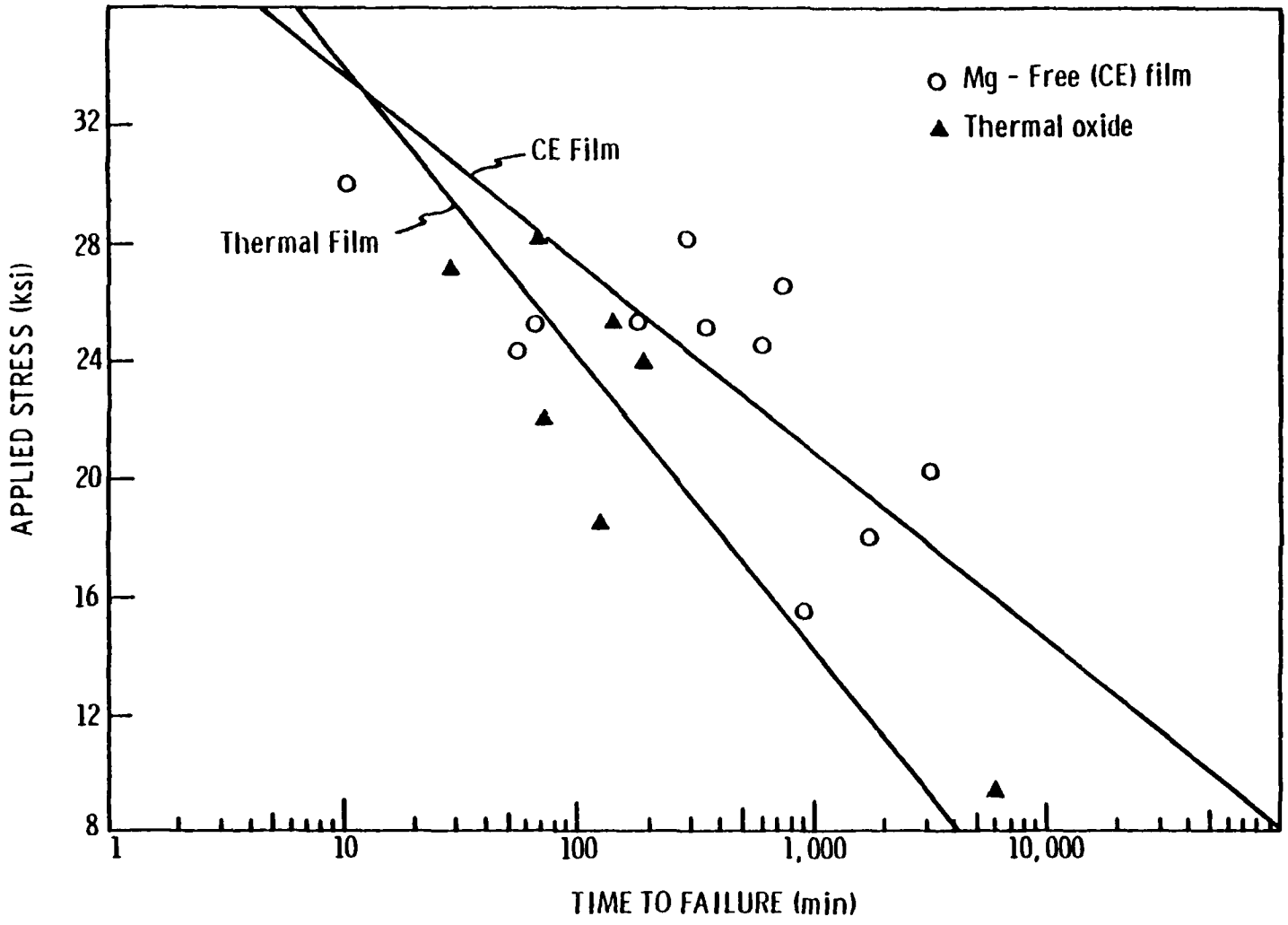

Figure 7. Stress vs time to failure for alloy B. Specimens treated with the caustic etching procedure have decreased susceptibility.

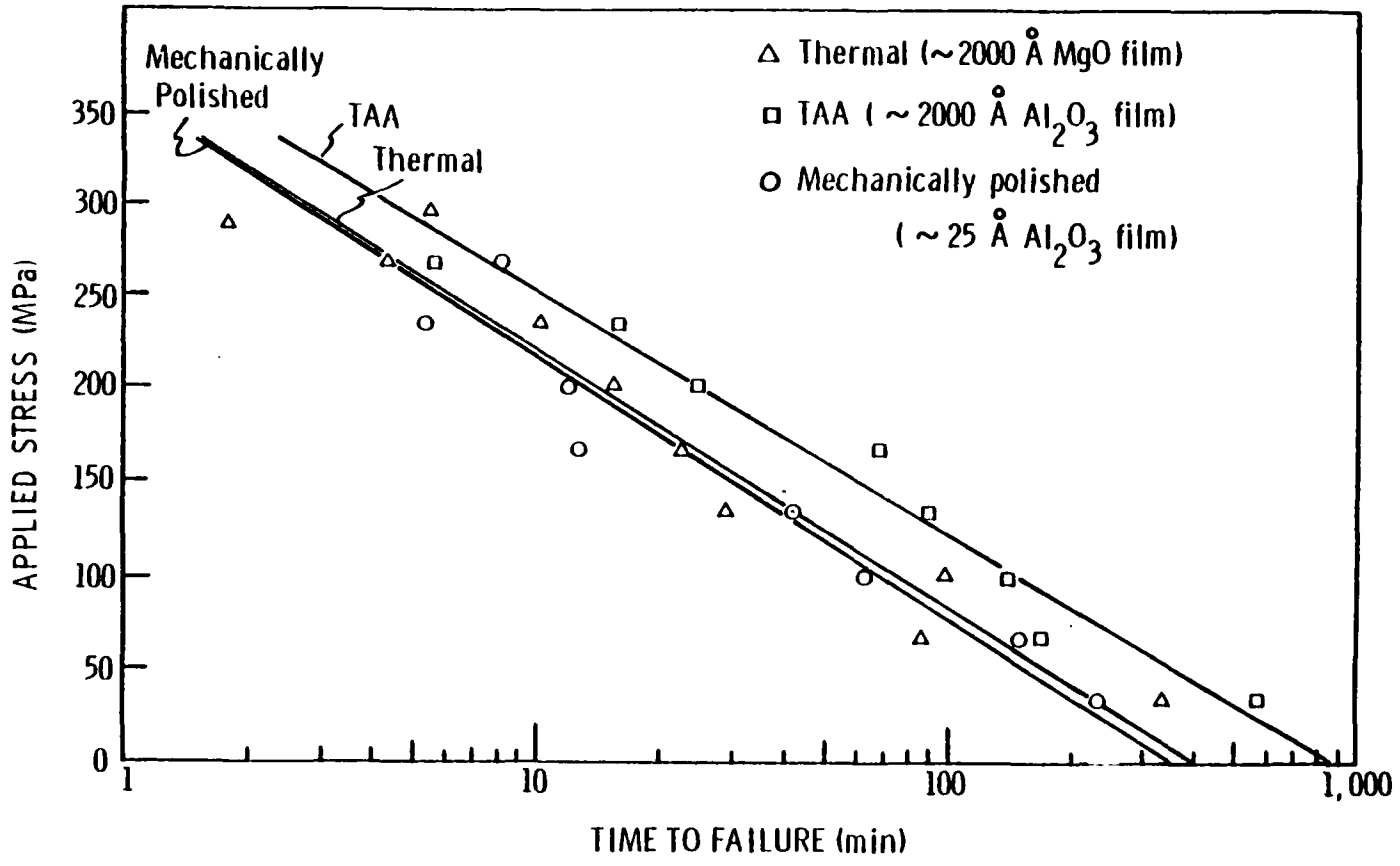

Figure 8. Stress vs time to failure for thermal and Mg-free films on alloy G.

3. Discussion

All of the film removal procedures successfully removed the Mg-rich, "thermal" oxide and replaced it with a Mg-free film formed at room temperature. The harmful effects of Mg in the film become apparent when one observes that a 25-Å, Mg-free film (as polished after heat treating) affords virtually the same protection as a 2,000-Å thermal film. Moreover, a TAA film (Mg-free) that is 2,000 Å thick affords approximately two times as much protection against SCC as a thermal film of the same thickness.

The CE data on alloy B show scatter, which is attributed to porosity in the starting ingot that carried over to the rolled sheet.[18] Despite the scatter, it is apparent that the CE procedure does reduce SCC susceptibility.

Of the three film removal procedures (CE, polishing, and polishing + TAA), CE may have commercial possibilities. (Polishing is obviously not commercially feasible.) Commercial 7xxx alloys could be given the CE procedure after heat treating to reduce their susceptibility to SCC initiation. This would simply entail immersing the fabricated part in several etching and rinse baths. Commercial forging plants often immerse forgings in acid baths[29] after heat treating to improve surface lustre for cosmetic reasons. We feel that this also may increase resistance to SCC initiation.

To see if the CE procedure can reduce the susceptibility of a commercial 7xxx alloy, we purchased 0.050-in.-thick, commercial 7075 sheet, machined sheet tensile specimens from it, and heat treated them to the T6 temper. Specimens were then tested in tension in acetic acid-brine, half having the thermal film, and the other half given the CE procedure and then loaded in tension in acetic acid-brine. Stress vs ttf data for this test are in Fig. 9.

There appears to be no difference in susceptibility between the two groups. This result can be explained by the grain size and orientation of the 7075 sheet. The grains had a mean-linear-intercept grain

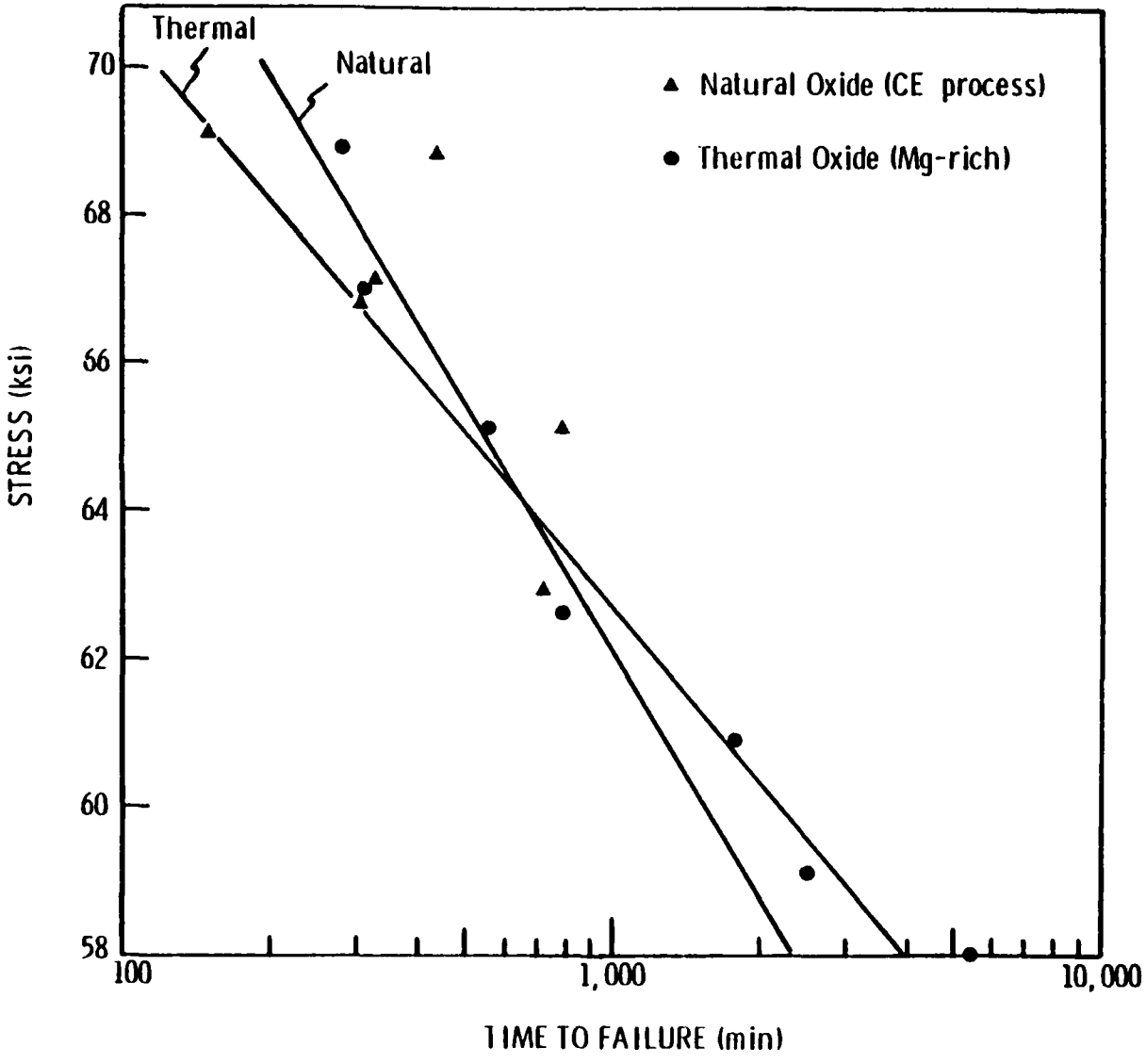

Figure 9. Stress vs time to failure for commercial 7075, showing the effect of the Mg-rich and CE-formed oxide. The grain orientation was such that the alloy was not susceptible to SCC and failed by pitting corrosion.

size of 41 x 41 um, 36 x 12 um, and 41 x 17 um on sections perpendicular to the short-transverse, long-transverse, and longitudinal directions, respectively (see Fig. 10). The specimens were machined parallel to the long-transverse direction, the most susceptible orientation possible,[30] given the limited thickness of the sheet. Because the crack tends to propagate in the longitudinal direction, it does not see favorably oriented grains that can easily separate by intergranular attack. Thus, the grain orientation is not suited for SCC, and microstructural examination has shown that the fracture path on these specimens is not intergranular. Fracture appears to have originated through pitting corrosion, which caused local stress concentration leading to failure. Thus, this experiment is inconclusive as to whether or not the CE process decreases SCC susceptibility of commercial 7075. We recently purchased 7075 with a more susceptible grain orientation and are repeating the experiment.

The CE procedure was not used successfully on extremely coarse-grained materials. The grain boundary-surface intersections on coarse-grained alloys are rapidly attacked by the caustic, resulting in grain-boundary grooving. These grooves serve as local stress-raisers, which cause fracture at shorter times at a given stress level. Figure 11 shows grain-boundary grooving of alloy G, which has a mean grain size of ~ 170 um.

The fact that the CE procedure does not appear to be successful in improving the SCC resistance of coarse-grained alloys does not limit its potential commercial usefulness because virtually all 7xxx commercial alloys are fine grained.

4. Oxide Characterization

We have attributed the higher susceptibility of specimens with thermal films over specimens with Mg-free films to magnesium content of the thermal film. However, since film porosity and/or differences in

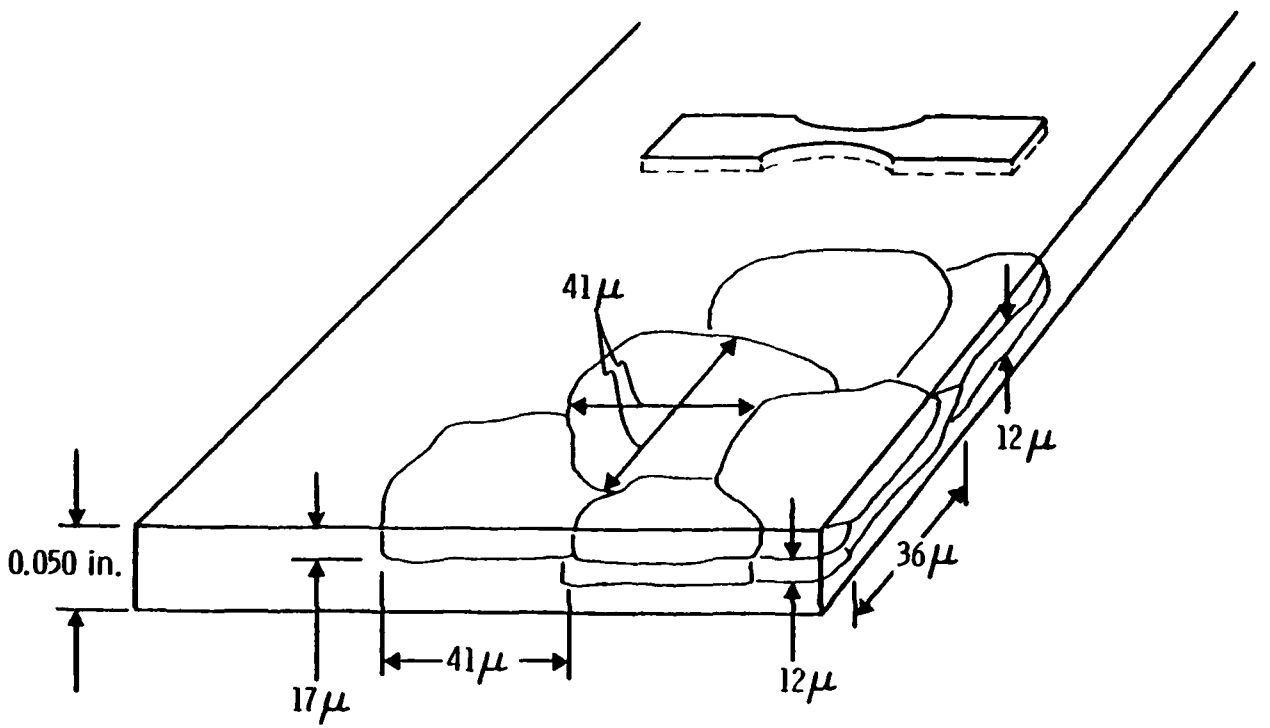

Figure 10. Grain orientation of commercial 7075 sheet.

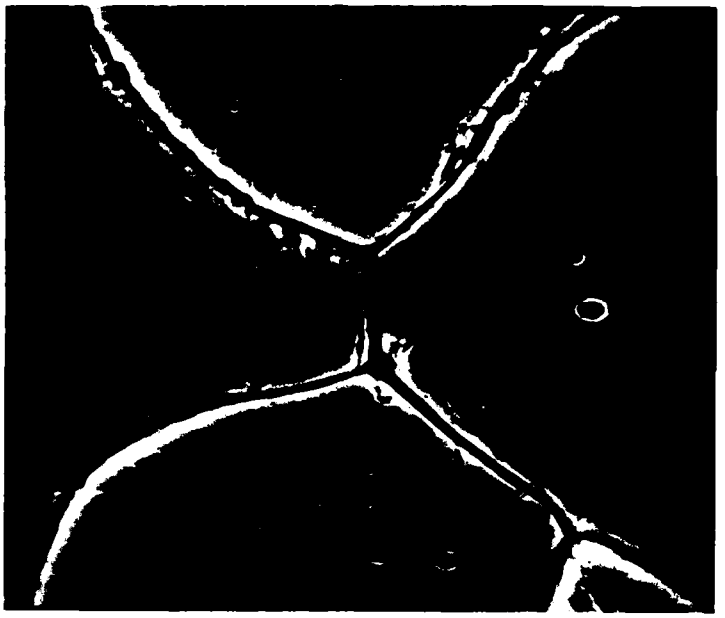

Figure 11. Grain boundary grooving following treatment of alloy G by the CE process. (Magnification 300x.)

purely mechanical, film-cracking behavior may also explain the differences, we performed the following two experiments. First, in the scanning mode of the STEM, we observed two specimens of alloy G, one having a 2,000-Å thermal film and the other, a 2,000-Å TAA film. Second, we loaded two similar specimens to the yield strength in air, unloaded them, and then examined them in the STEM for evidence of purely mechanical cracking.

The thermal film was quite porous (see Fig. 12a), having pores on the order of 2 μm in diameter, spaced about 10 μm apart. This porosity is probably caused by Mg evaporation that occurs during solution-heat treatment. In contrast, the TAA film was essentially pore free (Fig. 12b). At very high magnification, the TAA film appears to have fine porosity (see Fig. 13). However, a section including the profile of the TAA oxide reveals that pores are not present. The TAA film is wavy (Fig. 6), almost sinusoidal, and the downward undulations in the film look like pores when viewed normal to the surface. The thickness of the film is fairly constant.

Neither the thermal film nor the TAA film showed signs of mechanical cracking when observed in the STEM, unloaded after having been stressed to the yield strength in air. In fact, upon unloading, they appeared identical to Figs. 12a and 12b. Thus, differences in susceptibility likely are not due to differences in purely mechanical behavior of the films. This is consistent with the findings of Bubar and Vermilyea,[31] who demonstrated that aluminum films have surprising ductility. We do recognize that the films were not examined at high magnification under load, in which case cracking could be more readily detected. To do so would, of course, be technically very difficult.

Since the TAA film is less porous than the thermal film, the oxide morphology may also be responsible for the decreased susceptibility of specimens having the Mg-free film.

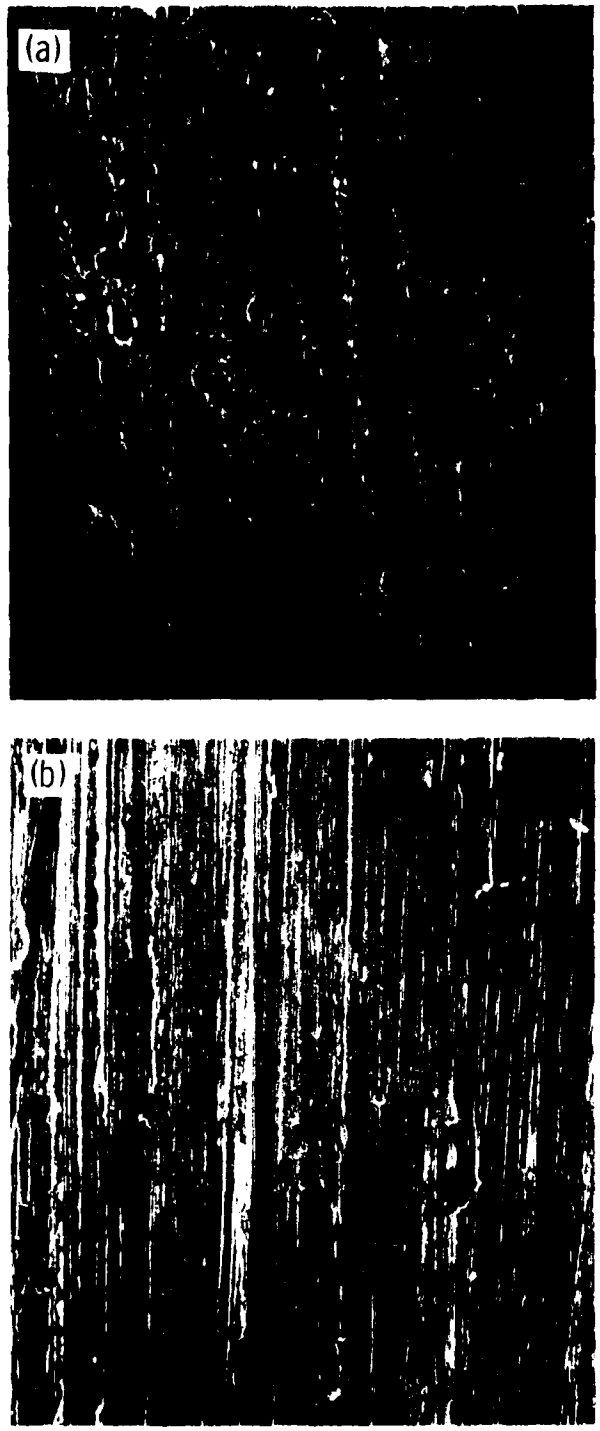

Figure 12. Scanning electron micrographs of (a) thermal oxide, and (b) TAA oxide. (Magnification 2,000x.)

Figure 13. High magnification scanning electron micrograph of TAA oxide showing undulation in the film (compare with Fig. 6). (Magnification 50,000x.)

5. Effect of Oxide Thickness

The previous experiments raise the question: what is the effect of oxide thickness on SCC susceptibility? It can be argued that a thicker film affords greater protection because penetration by chem-absorption is more difficult through a thicker film. On the other hand, one can argue that a thicker film has a higher probability of having a major flaw and will be more susceptible to purely mechanical cracking. Consequently, susceptibility to SCC may actually increase with film thickness by this a second model. To find answers to this question, specimens of alloy G were aged to peak hardness, mechanically polished, and anodized in tartaric acid. Films of various thicknesses were made by changing the anodizing voltage.[27,31] The specimens were loaded at 35 ksi (~ 75% YS) and placed in acetic acid-brine at room temperature.

Results of this experiment are shown in Fig. 14. The SCC susceptibility decreases (greater ttf) with increasing film thickness from 25 Å (no TAA, "natural film" only) to 2,000 Å. Skoulikidis and Karageorgos[32] found that SCC susceptibility of alloy Alcan 575 (5052) in saline solution increases with increasing anodizing film thickness. They used a 15 wt% H_2SO_4 bath as their anodizing reagent and produced films of γ Al_2O_3 that ranged in thickness from 3 to 28 μm. At each of the three stress levels investigated, SCC susceptibility increased as film thickness increased. They attributed this behavior to the greater number of structural defects that accompany thicker films and to these defects serving as initiation sites for pitting corrosion. Moreover, they claim that pitting corrosion is the first step in SCC initiation in their case.

Their result appears at first glance to be at odds with ours. However, Skoulikidis and Karageorgos[32] examined films ranging from 3 to 30 μm thick (30,000 to 300,000 Å), which is much greater than the 25- to 2,000-Å range examined in our current work. They do state that there will be different SCC behavior for films less than about 0.1 μm (1,000 Å) because films that are this thin have different sorption, aging, dissolution, and mechanical properties[31] than the γ Al_2O_3

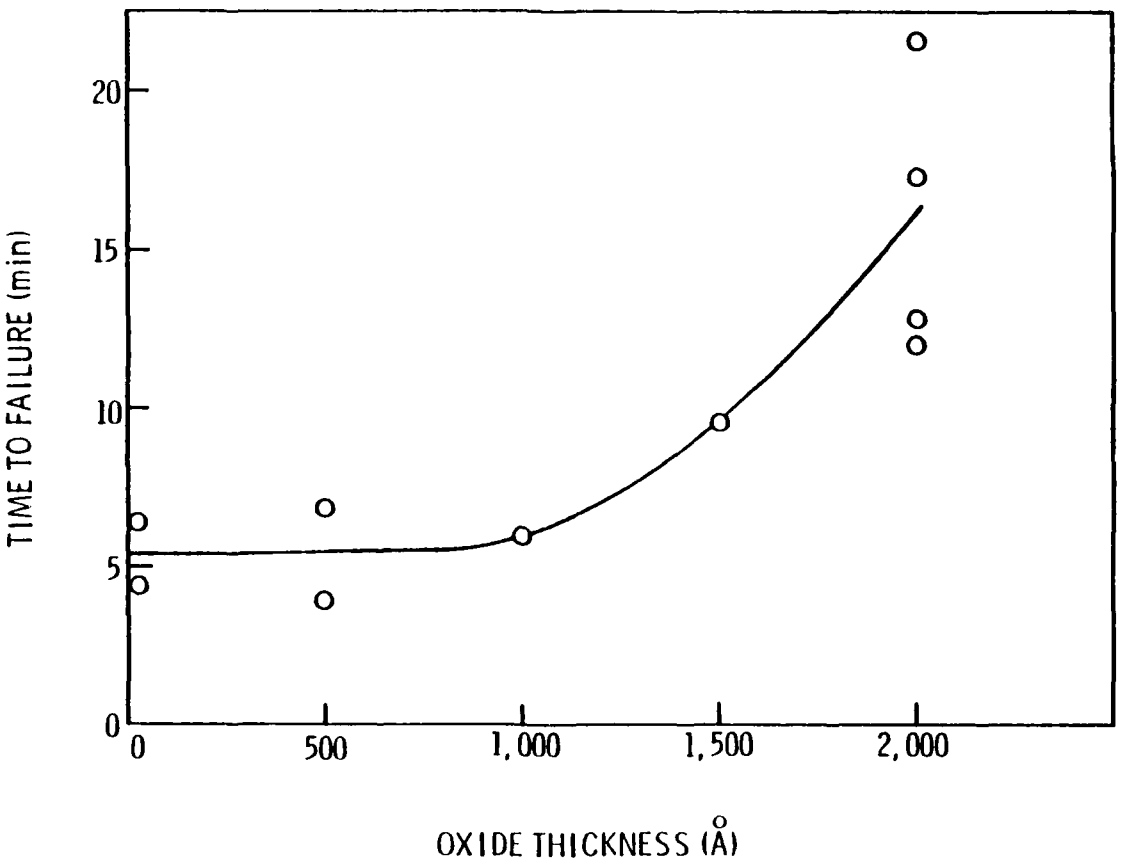

Figure 14. Time to failure vs TAA film thickness. Tested at constant stress in acetic acid-brine.

that formed by sulfuric acid anodizing. They speculated in their 1978 paper[32] that SCC will increase with increasing film thickness for films thinner than 0.1 μm. Their very recent work[33] contains data in this thickness regime that do show decreasing SCC susceptibility with increasing film thickness, which supports our results.

We must mention as an aside that Skoulikidis et al.[32-35] claimed to produce crystalline Al_2O_3 on the surface of aluminum. This has been tried unsuccessfully at the Laboratories using anodizing agents other than sulfuric acid.[36]

Our current results and those of Skoulikidis and Karageorgos[32,33] collectively suggest that SCC resistance (ttf in saline solution at a given stress) will increase with film thickness, go through a maximum, and then decrease. This behavior may be explained as follows. The film that initially forms on aluminum is amorphous Al_2O_3, which is nonporous and has good mechanical cracking resistance[32] (see section III.B.4). As the film thickness is increased by TAA, the amorphous nature of the film is maintained as is its relative freedom from porosity and freedom from mechanical cracking tendencies. As the film thickens by anodizing in sulfuric acid* or by reaction with moist air, the oxide becomes more porous,[32] and due to its greater thickness has a higher probability of having flaws. These thicker films can be penetrated by pitting, as claimed by Skoulikidis and Karageorgos,[32] or may simply crack mechanically under load.

C. EFFECT OF LOADING MODE

Green et al.[4] examined the effect of loading mode on SCC susceptibility of 7075 (Al-Zn-Mg-Cu) and showed that the cracking mechanism involves HE (see section II). This experiment aims to determine whether the 5xxx alloys (Al-Mg) also stress-corrode by a mechanism that involves HE and, if possible, to determine if magnesium content affects the tendency toward HE.

---

* We could not produce TAA films thicker than 2,000 Å.

1. Experimental Plan

We encountered many technical difficulties with this experiment, and expended a considerable amount of effort to establish the test systems. Many of these problems stem from the difficulty of obtaining suitable test materials. The 5xxx alloys typically have a moderate yield strength (YS) of 20-50 ksi, and an extensive search of the literature revealed no measurements of fracture toughness (K_{IC}) that meet strict test conditions. Previous results are denoted as "K_Q" because they have not satisfied fracture toughness test criteria. To ensure a valid fracture toughness test, the specimen dimensions must be greater than a minimum size to ensure that plane-strain conditions are met. Several such size criteria exist;[37,38] but, the conservative Brown and Srawley[38] criterion is widely used. This criterion states that the minimum specimen dimension "b" must be greater than a value computed from the YS and K_{IC} as follows:

$$b > 2.5\left(\frac{K_{IC}}{YS}\right)^2 \qquad (1)$$

Because YS is not very large for 5xxx alloys, the specimens may have to be quite large and of a high strength temper. Conceptually, this is not a problem because 5xxx alloys are only susceptible to SCC at high magnesium levels, which enhance strength. Moreover, to be susceptible, the alloys must be at tempers having a large amount of cold work or in an annealed condition that softens the alloy, which results in precipitation of the β phase (Mg_2Al_3) on the grain boundaries.[39] This latter condition is impractical for K_{IC} testing because "b" would be huge because YS is very small. Alloys with a high Mg content are available, but those with high strength tempers are rarely made in sections thick enough to satisfy the Brown and Srawley condition.

We obtained 3-in.-thick 5456 H116 plate, courtesy of the Naval Surface Weapons Center in Dahlgren, VA. The yield strength of this alloy was too low to make valid K_{IC} specimens of practical size. We then obtained 1.5-in.-thick 5083 H131 armour plate from Martin Marietta's Lewisport rolling mill. The tensile properties and grain size of this material were measured and are in Table 5. The fracture toughness of this alloy is unknown, but by estimating a value of 30 ksi $\sqrt{\text{in.}}$ for K_{IC} (similar to that of 7075) and using 41.8 ksi for the long transverse yield strength, the value of "b" computed from equation 1 was 1.29 in. The thickness dimension of the 5083 H131 plate, 1.5 in., is large enough to satisfy the Brown and Srawley condition if the assumed value of K_{IC} is reasonably correct.

a. Mode I specimens

The compact-tension (CT)[40] specimen geometry was selected for this test, and specimens were machined in the TL orientation[30] (Fig. 15) to increase the tendency toward SCC. We closely followed the recommended testing procedure for the CT specimen, ASTM E399 78. A chevron notch was used, and Fig. 16a is a schematic showing the dimensions of our specimen. Note that the minimum dimension "b" is 1.5 in. to provide a margin of safety over the Brown and Srawley criterion in case the estimated value of K_{IC} is low.

Specimens have been machined and are now being fatigue precracked in an MTS machine.

b. Mode III specimens

There is no accepted criterion for the minimum specimen dimensions under Mode III loading. One third of the Brown and Srawley criterion was taken as a rough guess for "b" in Mode III.

The specimen geometry selected for this work is a modification of the notched-cylindrical specimen developed by Hayden and Floreen[41] and

Table 5

Grain Size and Tensile Properties of 5083 H131

Grain axis:	Longitudinal	Long Transverse	Short Transverse
Grain diameter (μm):	275	100	15
0.2% yield strength (ksi):	41.8	41.0	---
Ultimate tensile strength (ksi):	49.1	50.8	---

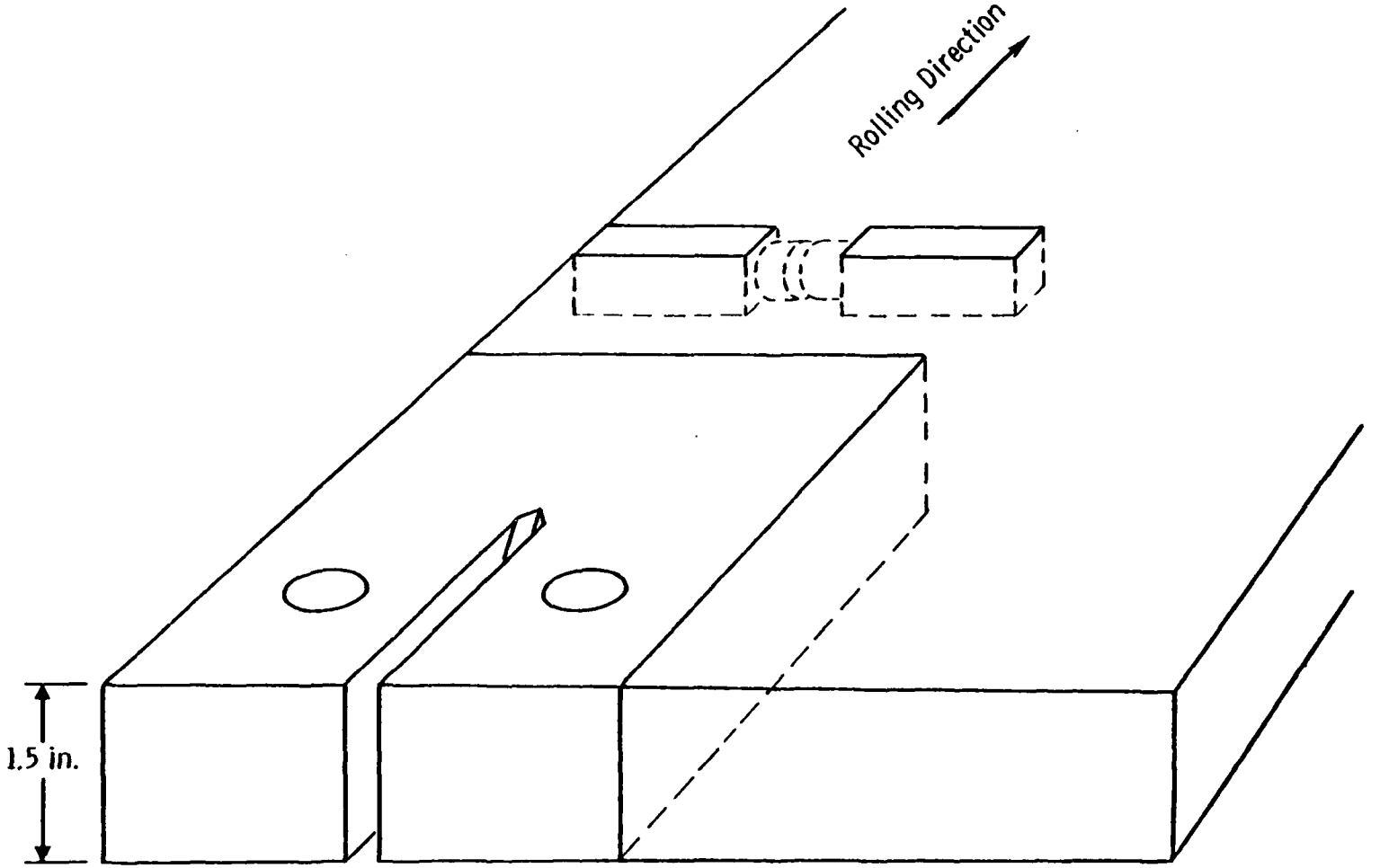

Figure 15. Orientation of compact tension and torsion specimens on 5083 plate.

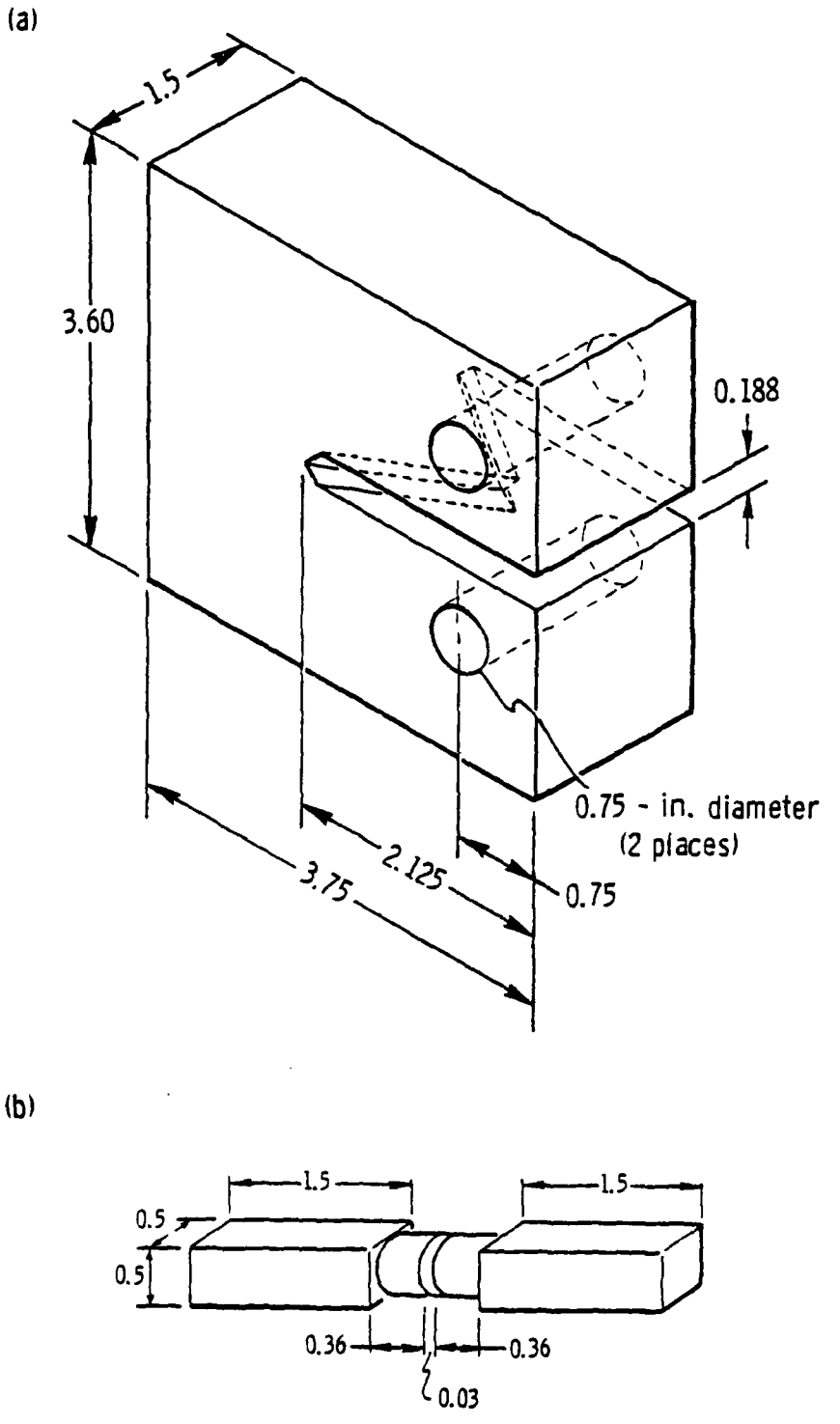

Figure 16. Schematic of (a) compact tension specimens (Mode I), and (b) Mode III specimens used in this program (dimensions in inches).

used by Green et al.[4] in their loading mode experiment. To make the test ligament thicker, the notch was machined to a shallower depth, 0.038 in. as compared with the 0.108 in. used by Green et al.[4] (see Fig. 16b). To make the stress state at the root of the notch more severe, the angle of this notch was decreased from 60° to 45°. Specimens were machined in the long-transverse orientation as shown in Fig. 15.

Green et al.[4] did not precrack their specimens. Precracking reduces scatter and aids in ensuring that the limiting toughness in Mode III loading, K_{IIIC}, can be obtained. Consequently, we decided to precrack the specimens. Using a lathe, we applied a moment perpendicular to the axis of rotation while the specimen to be precracked was spinning, thus causing the edge of the specimen to deflect. This deflection could be increased by advancing a calibrated threaded screw (see Fig. 17).

Precracking was successfully accomplished using a deflection of the edge of the specimen of 0.0475 in. for 10 min while the lathe was rotating at 150 rpm.

2. Results

The K_{IIIC} measured for the 5083 H131 was 11.0 ksi $\sqrt{\text{in.}}$ To our our knowledge, this is the first time K_{IIIC} has been reported for a 5xxx alloy.

3. Ongoing Toughness Testing

A corrosive solution cup is being fabricated, and K_{III} vs ttf data in an aqueous chloride-containing environment will be generated shortly.

The grips for the CT specimens are being machined. The CT specimens have been machined and will be fatigue precracked on an MTS machine. We will then perform a compliance calibration to enable precise, indirect measurement of crack length[42] and crack velocity. We will then measure K_{IC}.

Figure 17. Mode III precracking apparatus.

A corrosive solution cup is also being fabricated for the CT specimens to enable generation of K_I vs ttf data in the presence of corrosive solution.

D. IDENTIFICATION OF Mg-H COMPLEX BY AUGER PLASMON-LOSS SATELLITE PEAKS

In earlier work at Martin Marietta Laboratories, Sun et al.[12] found that by measuring the plasmon-loss energy (PLE) of the Mg Auger peaks, we could determine whether the Mg was bound (e.g., to Zn in $MgZn_2$) or chemically free. We used this technique to attempt to measure the PLE of Mg-H formed in the Auger chamber. We then planned to attempt to identify this compound on the fracture surface of stress-corroded Al-Zn-Mg by looking for the previously characterized Auger satellite peak.

1. Experimental Procedure and Results

A polished block of magnesium was placed in the Auger beam and cleaned by argon-ion bombardment under vacuum. High-resolution Auger electron spectra were generated before and after exposing the specimen to a) ambient H_2 (2×10^{-6} torr) for 20 minutes, and b) 2 KeV H^+ ion bombardment for 5 minutes. No satellite peak was detected after each exposure to hydrogen.

2. Discussion

This disappointing result means one of several things:

1) An Mg-H complex cannot form by this method.
2) The PLE of the satellite peak of the Mg-H complex is too small to be measured using existing equipment.
3) The Mg-H complex formed but decomposed so rapidly in the vacuum that its PLE could not be measured.

Two magnesium hydrides are known to exist: Mg-H and MgH_2. The former is extremely unstable, and consequently, is less likely to be detectable on a SCC fracture surface should it be involved in the SCC mechanism. The MgH_2 is more stable, and several papers describe its formation and characteristics.[43-45] From these papers, we found that MgH_2 becomes unstable at room temperature when exposed to vacuum. This poses extreme difficulties in detecting MgH_2 on SCC fracture surfaces because surface science tools that can detect small amounts of a material require examination under high vacuum.

As mentioned earlier, C.D.S. Tuck[15] used DSC to characterize MgH_2 and looked for its presence on the SCC fracture surface. J.R. Pickens met with him, and he provided us with MgH_2 powder. We planned to repeat the PLE experiment on MgH_2, measure the PLE, and look for its presence on the SCC fracture surface. However, Auger examination of the powder provided by Tuck revealed that it was hydrated and, therefore, could not be used for this experiment. We hope to repeat this experiment using noncontaminated MgH_2.

E. FRACTOGRAPHY

Considerable fractographic examination was performed to elucidate the fracture mechanism. Much of the work was done on alloy G because its coarse grain size facilitates microscopic examination.

1. Experimental Procedure

Specimens of alloy G were fractured in acetic acid-brine at room temperature. Immediately after fracture, the specimens were removed and rinsed in distilled water to prevent the fracture surface from pitting. In some cases, we examined the fracture surface plane, and in others, a plane normal to the fracture surface that contains the fracture-surface profile.

2. Results

The fracture path is largely intergranular, and a transition region from inter- to trans-granular was visible on alloy B,[18] which is fine grained. This region denotes the transition from SCC to purely mechanically-induced fast fracture. Pitting was generally observed on the surfaces of specimens loaded in acetic acid-brine. The pitting penetrated the oxide layer and attacked the metal substrate. The bottom of the pit was clearly intergranular (see Fig. 18). It appears that the pitting may initiate SCC because extensive intergranular cracking often proceeded from pits. The initiation mechanism may proceed as follows. The oxide film is the alloy's first defense against SCC. The corrosive solution penetrates the film by pitting and initiates intergranular SCC propagation. This intergranular attack may proceed to a significant depth below the main fracture plane. For example, Fig. 19 shows a fracture surface profile on a polished section with extensive attack beneath the main fracture plane. This attack often extends outward toward the surface oxide. Figure 20 at point (a) shows intergranular cracking below the main fracture plane that is visible <u>through</u> the surface oxide. Thus, the oxide is not penetrated from internal stress-corrosion cracks. This is evidence of the importance of the initiation stage of SCC.

Figure 20 shows the stress-corrosion crack propagating along the <u>sides</u> of the grain boundary [point (b)]. This is at first glance strange because the region adjacent to the grain boundary is solute-depleted, and therefore, should be cathodic with respect to the grain boundary region. Perhaps it is the region beyond the solute depleted zone that is dissolving. This region should be anodic with respect to the solute-depleted zone, and therefore, may preferentially dissolve.

Figure 18. Scanning electron micrograph showing severe pitting that initiates intergranular cracking. (Magnification 300x.)

Figure 19. Fracture surface profile of alloy G showing intergranular fracture. (Magnification 200x.)

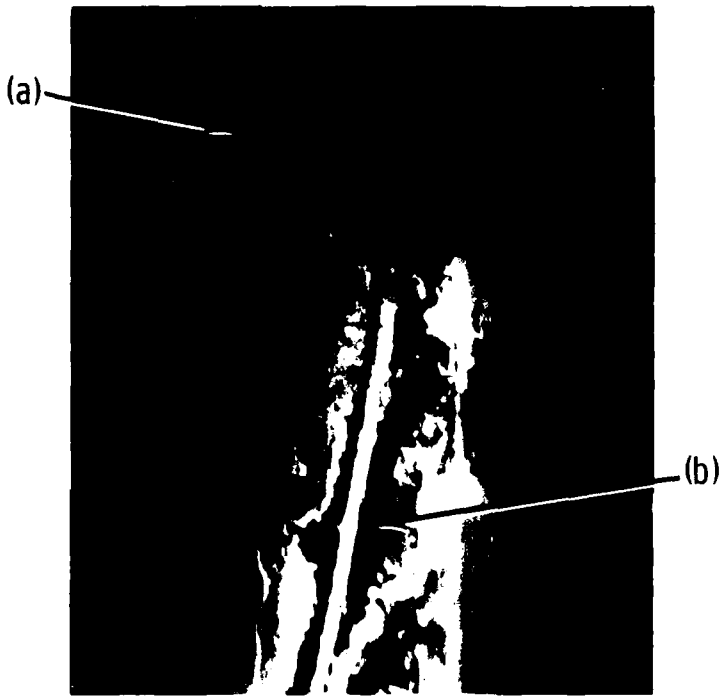

Figure 20. Fracture surface profile of alloy G showing (a) cracking visible beneath the film, and (b) intergranular cracking propagating adjacent to the grain boundary. (Magnification 1,000x.)

F. CONCLUSIONS

1. The SCC susceptibility of Al-Zn-Mg alloys in an aqueous, chloride containing environment increases with bulk solute content (wt% Mg + wt% Zn); and, for constant solute content within the composition range studied, susceptibility increases with increasing Mg/Zn.

2. Proper removal of the Mg-rich surface oxide-film that forms during solution heat-treatment reduced the SCC susceptibility of two Al-Zn-Mg alloys.

3. Susceptibility to SCC decreases with increasing thickness of tartaric-acid-anodized films in the range of 25 to 2,000 Å.

4. No signs of purely mechanical cracking were detected in either the Mg-rich thermal film or the Mg-free film (formed by anodizing in tartaric acid) when they were loaded to the yield stress in air.

5. The Mg content of the surface oxide-film, and possibly its porosity, play a role in the SCC initiation mechanism in Al-Zn-Mg alloys having oxide films that form during solution heat-treatment.

6. Pitting corrosion can cause SCC initiation in Al-Zn-Mg alloys.

IV. REFERENCES

1. E.N. Pugh, J.A.S. Green, and A.J. Sedriks: "Current Understanding of Stress Corrosion Phenomena," in Proc. Int. Conf. on Interfaces, August 1969, pp. 237-256. Also RIAS Tech. Rept. 69-3, Baltimore, MD.

2. A.J. Sedriks, J.A.S. Green, and D.L. Novak: "On the Chemistry of the Solution at Tips of Stress Corrosion Cracks in Al Alloys," Corrosion NACE, 1971, vol. 27, no. 5, p. 198.

3. A.J. Sedriks, J.A.S. Green, and D.L. Novak: "The Influence of the Heat Treatment on the Stress Corrosion Susceptibility of a Ternary Al-Zn-Mg Alloy," Metall. Trans., 1973, vol. 4, p. 1992.

4. J.A.S. Green, H.W. Hayden, and W.G. Montague: "The Influence of Loading Mode on the Stress Corrosion Susceptibility of Various Alloy/Environment Systems," in Proc. Conf. on Effect of Hydrogen on Behavior of Materials, p. 200, edited by A.W. Thompson and I.M. Bernstein (AIME, Philadelphia, PA, 1976).

5. L. Montgrain and P.R. Swann: "Electron Microscopy of Hydrogen Embrittlement in a High Purity Al-Zn-Mg Alloy," in Hydrogen in Metals, p. 575, edited by I.M. Bernstein and A.W. Thompson (ASM, Materials Science Division, Metals Park, OH, 1974).

6. R.J. Gest and A.R. Troiano: "Stress Corrosion and Hydrogen Embrittlement in an Aluminum Alloy," Corrosion, 1974, vol. 30, no. 8, p. 274.

7. M.O. Speidel: "Hydrogen Embrittlement of Aluminum Alloys?" in Hydrogen in Metals, p. 23, edited by I.M. Bernstein and A.W. Thompson (ASM, Materials Science Division, Metals Park, OH, 1974).

8. R. Alani and P.R. Swann: "Water Vapour Embrittlement and Hydrogen Bubble Formation in Al-Zn-Mg Alloys," Br. Corros. J., 1977, vol. 12, No. 2, p. 80.

9. C. St. John and W.W. Gerberich: "The Effect of Loading Mode on Hydrogen Embrittlement," Metall. Trans., 1973 vol. 4, p. 589.

10. J.A.S. Green, R.K. Viswanadham, T.S. Sun, and W.G. Montague: "Grain Boundary Segregation and Stress Corrosion Cracking of Aluminum Alloys," in Corrosion/77, Proc. Int. Corrosion Forum , Paper 17, p. 17/1 (Natl. Assoc. Corros. Eng., San Francisco, CA, 1977).

11. R.K. Viswanadham, T.S. Sun, and J.A.S. Green: "Grain Boundary Segregation in Al-Zn-Mg Alloys -- Implications to Stress Corrosion Cracking," Metall. Trans. A, 1980, vol. 11A, p. 85.

12. T.S. Sun, J.M. Chen, R.K. Viswanadham, and J.A.S. Green: "Plasmon-Loss Satellites in Auger Spectra of Alloy Surfaces," Appl. Phys. Lett., 1977, vol. 31, no. 9, p. 580.

13. R.K. Viswanadham, T.S. Sun, and J.A.S. Green: Influence of Moisture Exposure on the Composition of Oxides on Al-Zn-Mg Alloy: An Auger Electron Spectroscopy Study," Corrosion, 1980, vol. 36, no. 6, p. 275.

14. G.M. Scamans, R. Alani, and P.R. Swann: "Pre-exposure Embrittlement and Stress Corrosion Failure in Al-Zn-Mg Alloys," Corros. Sci., 1976, vol. 16, no. 7, p. 443.

15. C.D.S. Tuck: "Evidence for the Formation of Magnesium Hydride on the Grain Boundaries of Al-Mg and Al-Zn-Mg Alloys During Their Exposure to Water Vapour," to be published in Proc. 3rd Int. Conf. on the Effect of Hydrogen on the Behavior of Materials, Jackson Lake, WY, August 26-29, 1980.

16. E. Hidvégi and E. Kovács-Csetényi: "Study on the Mechanism of Evaporation of Mg and Zn From Al-Zn-Mg Alloys," in Proc. 5th Int. Conf. on Thermal Analysis, p. 104-107, edited by H. Chihara, Osaka University, Japan (Heyden & Son, Ltd., London, 1977).

17. W. Pistulka and G. Lang: "Accelerated Stress-Corrosion Test Methods for Al-Zn-Mg Type Alloys," Aluminium, Duesseldorf, 1977, vol. 53, no. 6, p. 366.

18. J.R. Pickens, D. Venables, and J.A.S. Green: "The Delayed Fracture of Aluminum Alloys," Report for ONR contract N00014-74-C-0277, P00006, May 1980.

19. J.R. Pickens, D. Venables, and J.A.S. Green: "Improved SCC Resistance of Al-Zn-Mg Alloys by Control of Mg Content in the Bulk Metal and In the Oxide Film," to be published in Proc. 3rd Int. Conf. on the Effect of Hydrogen on the Behavior of Materials, Jackson Lake, WY, August 26-29, 1980.

20. L.F. Mondolfo: Aluminum Alloys Structures and Properties, pp. 844-ff (Buffersworth, London, 1976).

21. B.K. Saxena, K. Lal, C.S. Sivaramakrishman, and R. Kumar: "Influence of Processing Variables on the Stress Corrosion Characteristics of Weldable Al-Zn-Mg Alloys," Light Met. Age, 1979, vol. 37, pp. 24-29.

22. P.R. Swann: Discussion in Hydrogen in Metals, p. 274, edited by I.M. Bernstein and A.W. Thompson (ASM, Materials Science Division, Metals Park, OH, 1974).

23. J.T. Staley: "Stress-Corrosion Cracking in Aluminum Alloys," Met. Eng. Q., 1973, vol. 13, no. 4, pp. 52-57.

24. J.T. Staley, Alcoa Technical Center, private communication to J.R. Pickens, Martin Marietta Laboratories, August 14, 1980.

25. R.I. Ganguly and B.K. Dhindaw: "Effect of Alloying Elements on the Stress Corrosion Failure of Al-Zn-Mg-Cu Alloys, Studied by Regression Analysis Technique," Br. Corros. J., 1977, vol. 12, no. 4, p. 239.

26. P.R. Sperry and M.H. Bankard: ASM Metals Handbook, vol. 8, 8th edition, p. 120 (ASM Publication, Metals Park, OH, 1973).

27. J.C. Grosskreutz and G.G. Shaw: "Structure of Anodic Layers on the (100) Face of Aluminum," J. Appl. Phys., 1964, vol. 35, no. 7, pp. 2195-2197.

28. D.A. Vermilyea: "Stresses in Anodic Films," J. Electrochem. Soc., 1963, vol. 110, no. 4, p. 345.

29. C. Maciejewski, Martin Marietta Aluminum, Torrance, CA, private communication to J.R. Pickens, Martin Marietta Laboratories, 1980.

30. B.F. Brown: Chapter 1 of Stress Corrosion Cracking Control Measures, NBS Monograph 156, pp. 1-34 (U.S. Dept. of Commerce, National Bureau of Standards, Washington, DC, 1977).

31. S.F. Bubar and D.A. Vermilyea: "Deformation of Passive Films," J. Electrochem. Soc., 1967, vol. 114, no. 9, p. 882.

32. Th. Skoulikidis and Ath. Karageorgos: "Protection of Aluminium Alloys Against Stress Corrosion Cracking in Saline Water by Properly Oriented Anodic Coatings, II. Influence of γ_1 Oxide Thickness," Br. Corros. J., 1978, vol. 13, no. 1, p. 28.

33. Th. Skoulikidis and Ath. Karageorgos: "Protection of Aluminium Alloys Against Stress Corrosion Cracking in Saline Water by Properly Oriented Anodic Coatings, III: Influence of $\gamma_{1,2}$-Al_2O_3 and γ_2-Al_2O_3 Oxide Thickness; Correlation Between Sorptive (and or Catalytic) and Protective Properties of Various Oxides," Br. Corros. J., 1980, vol. 15, no. 1, p. 41.

34. Th. Skoulikidis and Ath. Karageorgos: "Protection of Aluminium Alloys Against Stress Corrosion Cracking in Saline Water by Properly Oriented Anodic Coatings, I: Influence of Anodizing Conditions," Br. Corros. J., 1975, vol. 10, no. 1, p. 17.

35. Th. Skoulikidis, Ath. Karageorgos, and G. Batis: "Contribution to the Interpretation of the Formation of the Active Path in Stress Corrosion Cracking of Aluminum Alloys, I: Indirect Evidence From Electrolytically Notched Specimens," Br. Corros. J., 1976, vol. 11, no. 3, p. 143.

36. J.D. Venables, Martin Marietta Laboratories, private communication to J.R. Pickens, Martin Marietta Laboratories, 1980.

37. J.F. Knott: Fundamentals of Fracture Mechanics, p. 149 (John Wiley and Sons, NY, 1973).

38. W.F. Brown, Jr., and J.E. Srawley: Plane Strain Crack Toughness Testing of High Strength Metallic Materials, ASTM special technical publication no. 410, ASTM, Philadelphia, PA, 129 pp., 1966.

39. D.O. Sprowls and R.H. Brown: "Stress Corrosion Mechanism for Aluminum Alloys," in Proc. Conf. on Fundamental Aspects of Stress Corrosion Cracking, pp. 466-506, discussion 506-512, edited by R.W. Staehle, A.J. Forty, D. Van Rooyer (Ohio State University Press, Columbus, 1969).

40. "Standard Method for Test for Plane-Strain Fracture Toughness of Metallic Materials," in 1980 Annual Book of ASTM Standards, Part 10: Metals -- Physical, Mechanical, Corrosion Testing, ASTM Philadelphia, PA, pp. 580-601, 1980.

41. H.W. Hayden and S. Floreen: "Effects of Various Modes of Loading on the Stress Corrosion Cracking of a Maraging Steel," Corrosion NACE, 1971, vol. 27, no. 10, pp. 429-433.

42. H.R. Smith and D.E. Piper: "Stress-Corrosion Testing with Pre-cracked Specimens," Part 2, Boeing, Seattle, WA, sponsored by ARPA, No. 878, pp. 7-10, Draft June 1970.

43. T. Schober: "The Magnesium-Hydrogen System: Transmission Electron Microscopy," to be published, Institut für Festkörperforschung Kernforschungsanlage Jülich, 5170 Jülich, Germany.

44. T.N. Dymova, Z.K. Sterlyadkina, and V.G. Safronov: "Preparation of Magnesium Hydride," Russian J. Inorg. Chem., April 1961, p. 389.

45. R.H. Wiswall, Jr., and J.J. Reilly: "Metal Hydrides for Energy Storage," Brookhaven National Laboratories, Upton, NY, 11973, 729210.

APPENDIX A

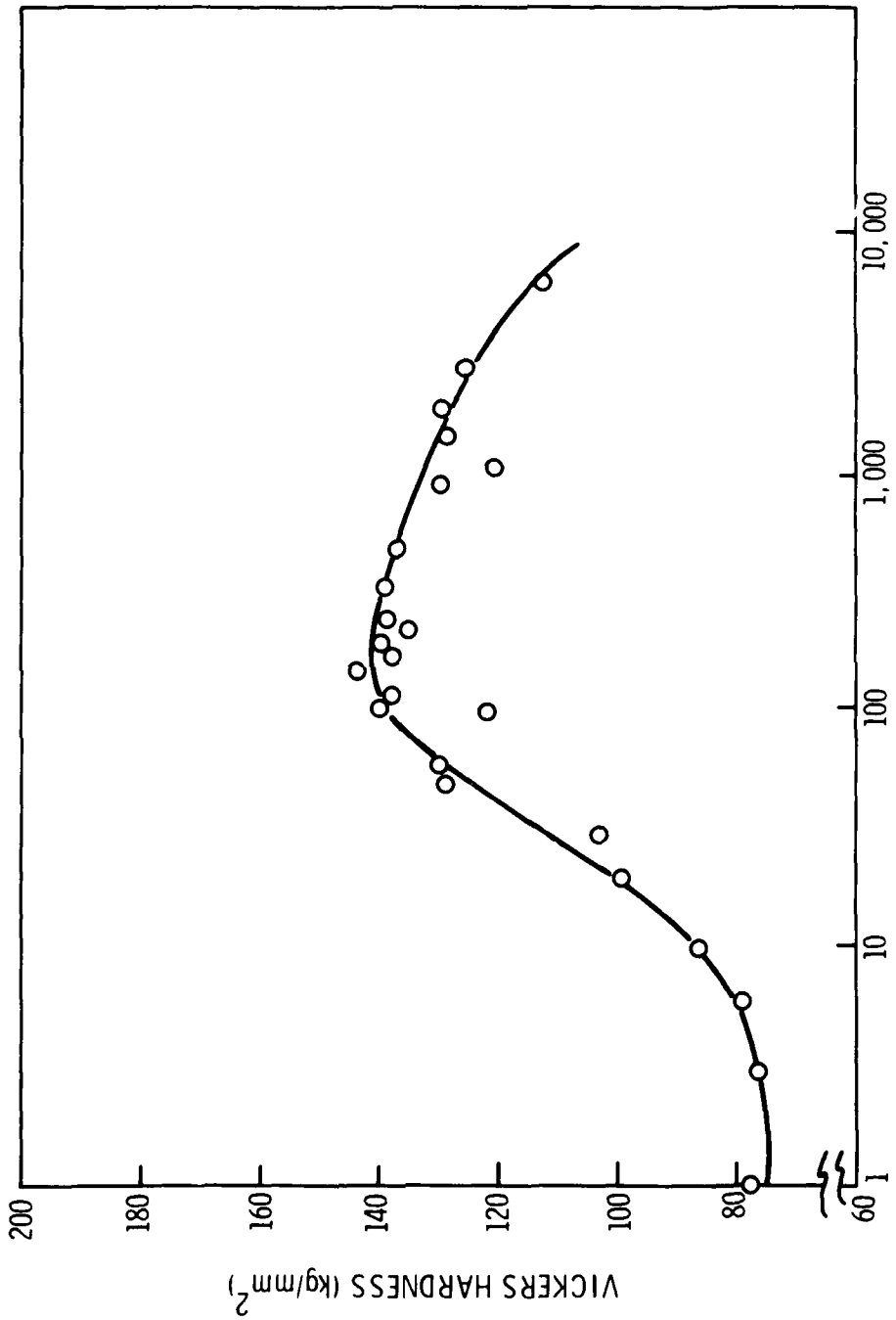

Figure A-1. Vickers hardness vs aging time at 150°C for alloy G.

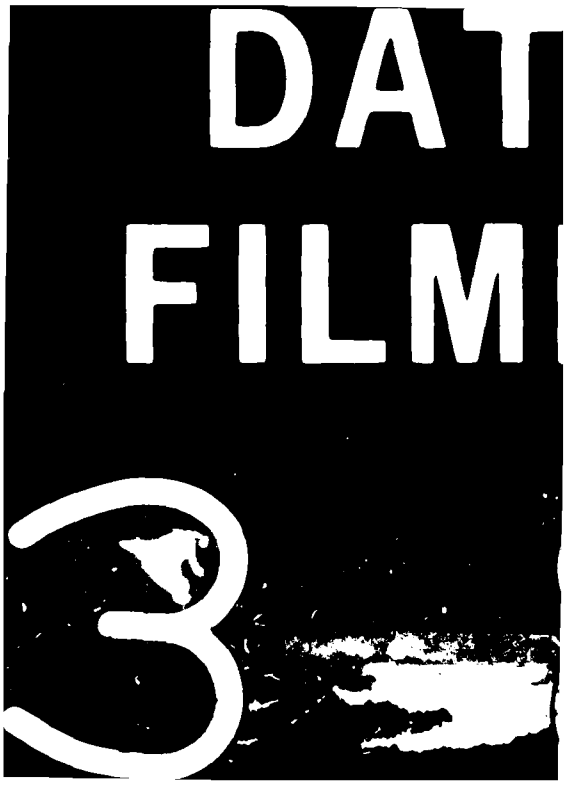
DAT
FILM